

Quantitative Estimation of the Efficiency of Electron Injection from Excited Sensitizer Dye into Nanocrystalline ZnO Film

Toshitada Yoshihara,[†] Ryuzi Katoh,^{*,‡} Akihiro Furube,[†] Miki Murai,[†] Yoshiaki Tamaki,^{†,§} Kohjiro Hara,[†] Shigeo Murata,[†] Hironori Arakawa,[†] and M. Tachiya[§]

Photoreaction Control Research Center (PCRC), National Institute of Advanced Industrial Science and Technology (AIST), Tsukuba Central 5, 1-1-1 Higashi, Tsukuba, Ibaraki 305-8565, Japan

Received: September 30, 2003; In Final Form: December 2, 2003

The absolute value of the efficiency of electron injection from an excited coumarin dye (NKX-2311) into a nanocrystalline ZnO film was estimated as 0.8 ± 0.1 through transient absorption measurements. This value was obtained by using the molar absorption coefficient of the oxidized form of NKX-2311 determined in solution. Using this value and the previously obtained relative injection efficiency, we estimated the molar absorption coefficients of the oxidized form of N3 dye (*cis*-bis(4,4'-dicarboxy-2,2'-bipyridine)dithiocyanato ruthenium(II); Ru(dcbpy)₂(NCS)₂) and the conducting electrons in the ZnO film.

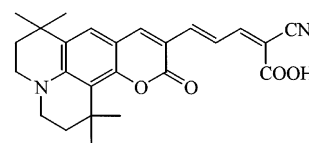
Introduction

Dye-sensitized solar cells consisting of N3 dye (*cis*-bis(4,4'-dicarboxy-2,2'-bipyridine)dithiocyanato ruthenium(II); Ru(dcbpy)₂(NCS)₂) adsorbed on nanocrystalline TiO₂ film have received much attention since Grätzel and co-workers achieved a high solar energy-to-electricity conversion efficiency ($\eta = 10\%$ under AM 1.5 irradiation) in 1993.¹ However, despite much effort to develop high-performance solar cells, no dramatic improvement in efficiency has been achieved. We have tried to develop highly efficient dye-sensitized solar cells with new Ru-complexes^{2,3} and organic sensitizer dyes.^{4–7} For solar cells with the new coumarin dye NKX-2311 (Scheme 1) adsorbed on nanocrystalline TiO₂ film (abbreviated NKX-2311/TiO₂), we achieved $\eta = 6\%$.⁵

The electron injection process is considered to be an important primary process in dye-sensitized solar cells. To realize high-performance solar cells, a high efficiency of electron injection from the excited sensitizer dye into the nanocrystalline semiconductor film is imperative. To evaluate the injection process, transient absorption spectroscopy has been widely applied. In the femtosecond time range, electron injection dynamics can be probed directly.^{8–23} Electron injection takes place very rapidly in the 0.1–100 ps time range in TiO₂,^{8–15,21} ZnO,^{16–18,21} and SnO₂,^{19–23} which implies that the efficiency of electron injection is very high because the rate of injection is much faster than the rate of fluorescence decay of the sensitizer dye, which is typically 10 ns.

The efficiency of injection has been evaluated through nanosecond transient absorption spectroscopy by monitoring the absorption due to the oxidized form of the sensitizer dye produced by the injection.^{24–28} Meyer and co-workers reported the effect of the concentration of ions in the surrounding solution on the efficiency.^{24,25} Recently, we determined the relative efficiency of electron injection by observing the absorption due to conducting electrons in the near-IR wavelength range (1000–3000 nm)²⁶ and evaluated the dependence of the efficiency on the free energy change for the electron injection. We also

SCHEME 1. Molecular Structure of NKX-2311



NKX-2311

determined the relative injection efficiencies for derivatives of Ru–phenanthroline complexes adsorbed on TiO₂ films and found that a molecule having one carboxyl group exhibited a very low efficiency compared with a molecule having four carboxyl groups.²⁷ From the analysis of the transient absorption signal, we concluded that there are two modes (one active for electron injection, and the other inactive) of adsorption of the molecule on the TiO₂ surface. We also studied the formation of inactive molecular aggregates.²⁸ For N3 dye adsorbed on ZnO, we observed the formation of micrometer-sized crystals of a complex between N3 and Zn²⁺, which were inactive for electron injection.

To discuss the injection process in detail, it is important to quantitatively analyze the efficiency of injection; thus absolute values of the injection efficiency are required. However, precise absolute values of the injection efficiency have not been determined to date. In general, determining such values is not easy because the absolute values of the molar absorption coefficients of the transient species (the oxidized dye and the conducting electrons in the semiconductor) are difficult to estimate owing to their instability and short lifetimes. For dye-sensitized systems, there is another difficulty. Sensitizer dyes absorb photons over a wide wavelength range; thus the absorption spectra of the transient species frequently overlap those of the ground-state dye. Nevertheless, Meyer and co-workers tried to estimate the absolute value of injection efficiency by using a complicated analysis of nanosecond transient absorption measurements, but found that the value strongly depended on the intensity of the exciting light.^{24,25} We also found that the efficiency depends on the light intensity.²⁶ Thus, sensitizer dye molecules must be carefully selected, and measurements must be made under weak excitation conditions. As mentioned above, relative values of the injection efficiency

* Corresponding author. E-mail: r-katoh@aist.go.jp.

[†] PCRC, AIST.

[‡] NEDO Fellow.

[§] AIST.

have already been obtained for some sensitizer dyes, so quantitative analysis can be realized if an absolute value is determined for a particular dye.

The absolute value of the efficiency Φ_{inj} of electron injection from an excited sensitizer dye into a semiconductor film can be expressed by

$$\Phi_{\text{inj}} = \frac{[N_{\text{ox}}]}{[N_{\text{photon}}]} = \frac{[N_{\text{electron}}]}{[N_{\text{photon}}]} \quad (1)$$

where $[N_{\text{ox}}]$ is the concentration of sensitizer in the oxidized state, $[N_{\text{electron}}]$ is the concentration of conducting electrons, and $[N_{\text{photon}}]$ is the number of absorbed exciting photons per unit volume. Through transient absorption measurements, $[N_{\text{ox}}]$ and $[N_{\text{electron}}]$ can be evaluated, and $[N_{\text{photon}}]$ can be determined from the intensity of the exciting light and the absorption spectra of the samples. Thus, Φ_{inj} can be rewritten in terms of the absorbance change due to generation of the oxidized form of the sensitizer dye (ΔA_{ox}), the absorbance change resulting from generation of the conducting electrons ($\Delta A_{\text{electron}}$), and the molar absorption coefficients ϵ of those species:

$$\Phi_{\text{inj}} = \frac{\Delta A_{\text{ox}}}{\epsilon_{\text{ox}}(1 - T)N_0} = \frac{\Delta A_{\text{electron}}}{\epsilon_{\text{electron}}(1 - T)N_0} \quad (2)$$

where T and N_0 represent the transmittance of excitation light and the number of incident excitation photons per unit area, respectively.

Here we estimate the absolute value of Φ_{inj} in NKX-2311/ZnO through transient absorption measurements. We used a highly sensitive transient absorption spectrometer developed previously and made our measurements under very weak excitation intensities. We estimated the absorption coefficient of the oxidized form of NKX-2311 from the electron-transfer reaction in solution. In addition, we discuss other systems and, in particular, estimate the absolute value of Φ_{inj} in N3/ZnO and the molar absorption coefficients of the oxidized form of the N3 dye and conducting electrons in the ZnO film.

Experimental Section

Benzoquinone (BQ, Wako) was purified by repeated recrystallization from ethanol. Methyl viologen trihydrate (MV^{2+} , Nacalai Tesque) was used as received. NKX-2311 was synthesized according to the reported procedure.⁵ Methanol (CH_3OH , Wako, spectroscopic grade) and methanol- d_4 (CD_3OD , Cambridge Isotope Laboratories, Inc., 99.8%) were used as solvents without further purification. A ZnO paste consisting of ZnO nanoparticles (Sumitomo Osaka Cement, #100), poly(vinyl acetal) (Sekisui Kasei, Bm-2) and α -terpineol was painted on a glass plate with a screen printer (Mitani Electronics Co., MEC-2400). Nanocrystalline films were prepared by calcination of the painted substrate for 1 h at 420 °C. The thickness of the films was about 5 μm , and the films were optically transparent. The apparent area of the ZnO films was about 1 cm^2 (1 cm \times 1 cm). The films were immersed in a solution of NKX-2311 in *tert*-butyl alcohol/acetonitrile (50:50) to fix the dye on the surface of ZnO particles. Samples dried in air were used for transient absorption measurements. All measurements were carried out just after the preparation of the samples to minimize the effect of dye degradation.

Absorption and fluorescence spectra were measured with an absorption spectrophotometer (Shimadzu, UV-3101PC) and a spectrofluorometer (Hitachi F-850), respectively. The fluorescence quantum yield Φ_f of NKX-2311 in CH_3OH was deter-

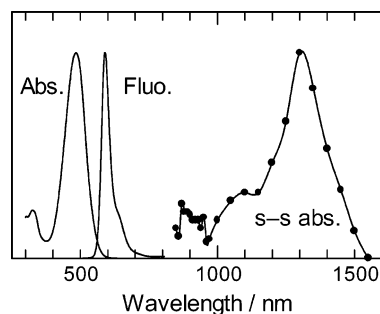


Figure 1. Absorption (Abs.) and fluorescence (Fluo.) spectra of NKX-2311 in CH_3OH . The singlet-singlet absorption (s-s abs.) spectrum of NKX-2311 in CD_3OD is also shown.

mined by comparing the integrated intensities of the fluorescence spectrum with those of Rhodamine 101 in ethanol ($\Phi_f = 1.0$).²⁹

For transient absorption measurements, the second harmonic (532 nm) of a Nd^{3+} :YAG laser (Spectra Physics, Pro-230-10) was employed for the excitation light source. The pulse duration was about 10 ns. A Xe flash lamp (Hamamatsu, L4642, 2 μs pulse duration) was used as the probe light source. For the measurements of solution, the probe light was focused in a 1 cm quartz cell containing solution, and the exciting light was incident perpendicular to the probe light. The concentration of CD_3OD solution of NKX-2311 was about 10^{-4} M. For the measurements of dye-sensitized films, the probe light was focused on the sample, and the exciting light was incident at 30° to the sample. The area irradiated with the exciting light (12 mm in diameter) covered the area probed by the probe light (4 mm in diameter). The probe light transmitted through the sample was introduced into a monochromator (JASCO CT-10 for the 600–950 nm range, Ritsu MC-10N for the 900–1400 nm range) after passing through the sample. The intensity change of the probe beam was detected by a Si photodiode (Hamamatsu, S-1722) in the 600–950 nm range and an InGaAs photodiode (Hamamatsu, G3476-05) in the 900–1400 nm range. The transient signals were recorded with a digital oscilloscope (Tektronix, TDS680C) and transferred to a personal computer for analysis. The intensity of the laser pulse was measured with a pyroelectric energy meter (Ophir, PE25). All measurements were carried out at 295 K.

Results and Discussion

The absorption spectrum of NKX-2311 in CH_3OH exhibits an absorption band with a maximum at 485 nm, and the fluorescence spectrum has a fluorescence band with a maximum at 590 nm (Figure 1). The fluorescence lifetime is 1.9 ns.⁴ The singlet-singlet absorption spectrum of NKX-2311 in CD_3OD exhibits a peak at 1300 nm (Figure 1). The fluorescence quantum yield was estimated to be 0.27, suggesting that excited triplet states are populated. However, we did not observe triplet-triplet absorption, implying that the triplet-triplet absorption is overlapped by the ground-state absorption.

To determine the absolute value of Φ_{inj} by eq 2, the molar absorption coefficient of the oxidized form of the dye is required. The oxidized form of NKX-2311 (NKX-2311^+) is produced by electron transfer from an excited NKX-2311 molecule to an electron acceptor in solution. We used BQ and MV^{2+} as the acceptors. The free energy change (ΔG) of the electron-transfer reaction can be expressed by

$$\Delta G = (eE_{\text{OX}} - eE_{\text{RED}}) - E_s \quad (3)$$

where E_{OX} is the oxidation potential of NKX-2311 (1.04 V vs

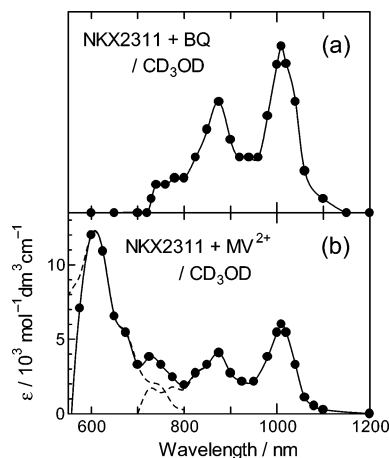


Figure 2. Transient absorption spectra of NKX-2311 in the BQ (a) and the MV²⁺ (b) solutions.

SCE in DMF⁴), E_{RED} is the reduction potential of BQ (−0.51 V vs SCE in acetonitrile³⁰) or MV²⁺ (−0.62 V vs SCE in water³¹), and E_{S} represents the energy of the singlet excited state of NKX-2311 (1.97 eV⁴). The values of ΔG for BQ and for MV²⁺ were negative (−0.42 and −0.31 eV, respectively). Therefore, electron transfer is expected to occur efficiently.

Figure 2 shows transient absorption spectra of CD₃OD solutions of NKX-2311 containing 0.10 M BQ (Figure 2a) or 0.10 M MV²⁺ (Figure 2b). These spectra were recorded 100 ns after 532-nm laser excitation. At this excitation wavelength, only the singlet excited state of NKX-2311 can be populated in the BQ and MV²⁺ solutions. For the BQ solution, the transient absorption band had peaks at 875 and 1010 nm. At 100 ns, the singlet excited states of NKX-2311 disappear because of their short lifetime (1.9 ns), and the spectrum at 100 ns is different from the singlet–singlet absorption spectrum shown in Figure 1. In this wavelength range, there is no absorption due to the BQ anion³² or the triplet–triplet absorption band of NKX-2311. Therefore, the spectrum shown in Figure 2a can be assigned to NKX-2311⁺, produced by electron transfer from excited NKX-2311 to BQ in CD₃OD. During measurement, we found that NKX-2311⁺ was stable over the range 0 to 1 μs , and degradation did not occur. It should be noted that the absorption spectrum of NKX-2311⁺ is not overlapped by the ground-state absorption of NKX-2311.

To estimate the molar absorption coefficient of NKX-2311⁺, we used MV²⁺ as an electron acceptor because the molar absorption coefficient of the oxidized form of MV²⁺ (MV⁺) was available. For the MV²⁺ solution, an absorption band with a maximum at 605 nm, which was assigned to MV⁺,³³ was observed in addition to the absorption spectrum of NKX-2311⁺ (Figure 2b). The spectrum obtained can be reproduced by adding the reported absorption spectrum of MV⁺ and the spectrum of NKX-2311⁺, as illustrated by the dashed lines in Figure 2b. The absorption spectrum of MV⁺ does not overlap with the spectra of NKX-2311⁺ and NKX-2311 around 600 nm, and there is no absorbance of MV⁺ at the 1010 nm maximum in the NKX-2311⁺ spectrum. Thus, using the value of the molar absorption coefficient of MV⁺ at 605 nm ($\epsilon_{605}^{\text{MV}^+} = 11900 \text{ mol}^{-1} \text{ dm}^3 \text{ cm}^{-1}$ ³⁴), we easily calculated the molar absorption coefficient of NKX-2311⁺ at 1010 nm ($\epsilon_{1010}^{\text{NKX-2311}^+}$) by the following relation:

$$\epsilon_{1010}^{\text{NKX-2311}^+} = \frac{\Delta A_{1010}^{\text{NKX-2311}^+}}{\Delta A_{605}^{\text{MV}^+}} \epsilon_{605}^{\text{MV}^+} \quad (4)$$

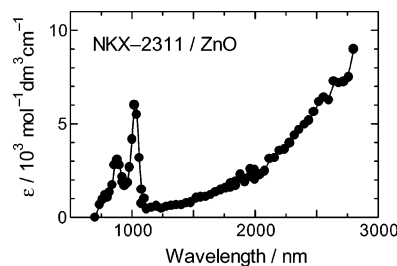


Figure 3. Transient absorption spectrum of NKX-2311/ZnO.

where $\Delta A_{1010}^{\text{NKX-2311}^+}$ and $\Delta A_{605}^{\text{MV}^+}$ are the absorbance change of NKX-2311⁺ at 1010 nm and the absorbance change of MV⁺ at 605 nm obtained through transient absorption measurements. The value of $\epsilon_{1010}^{\text{NKX-2311}^+}$ determined with eq 4 is $6000 \text{ mol}^{-1} \text{ dm}^3 \text{ cm}^{-1}$.

A few research groups have attempted to estimate the molar absorption coefficient of the oxidized form of the sensitizer dye in dye-sensitized solar cells. Several groups^{8,35–38} have studied the spectrum of the oxidized form of N3 dye, which is the most common sensitizer dye. Das and Kamat measured the spectrum of the oxidized form of N3 by reacting the dye with N₃⁺ and Br₂^{•+}.³⁵ They reported that the absorption spectrum of the oxidized form of N3 shows a peak at 740 nm in aqueous solution just after reaction and then exhibits a characteristic absorption maximum at 440 nm, corresponding to the formation of stable products. For this reason, analysis of the spectrum is rather difficult.^{36–38} Kelly et al. estimated the value of the molar absorption coefficient of the oxidized form of [bis(2,2'-bipyridine)][(4,4'-diethylester-2,2'-bipyridine)]ruthenium from the deviation of the ground state/excited-state isosbestic point from zero upon formation of the oxidized molecules.^{24,25} However, because of spectral overlap of the absorption bands, analysis of the spectrum is difficult. In the present case, NKX-2311⁺ is stable in solution, and the absorption band of the oxidized form does not overlap with the ground-state and excited-state absorption bands. Thus, we believe that NKX-2311 is a suitable molecule for reliably estimating the molar absorption coefficient of the oxidized form.

The transient absorption spectrum of NKX-2311/ZnO recorded immediately after 532-nm laser excitation exhibited peaks around 880 and 1020 nm (Figure 3). These peaks were assigned to NKX-2311⁺ on ZnO on the basis of the similarity with the absorption spectrum of NKX-2311⁺ in solution (Figure 2). The absorption peaks for NKX-2311⁺/ZnO are slightly red-shifted from those for NKX-2311⁺ in solution. This shift probably reflects the change in the molecular structure of NKX-2311 upon adsorption on the ZnO film. In the near-IR wavelength range, the absorbance increases monotonically with increasing wavelength. Absorption in the near-IR region is characteristic of conducting electrons in ZnO films²⁶ and is due to optical transition of electrons in the bottom of the conduction band to the upper levels of the conduction band (intraband transition).³⁹ These results indicate that electron injection from excited NKX-2311 into the conduction band of the ZnO film takes place efficiently.

Figure 4 shows decay profiles of the transient absorption signals of NKX-2311/ZnO at 1020 nm as a function of exciting light intensity I_{ex} . The transient absorption signal grows within the time resolution of the measurement system. The decay of the signal corresponds to charge recombination between NKX-2311⁺ and the conducting electrons and becomes slightly faster with increasing I_{ex} . This result is consistent with the rate of charge recombination in similar nanocrystalline films.⁴⁰ The

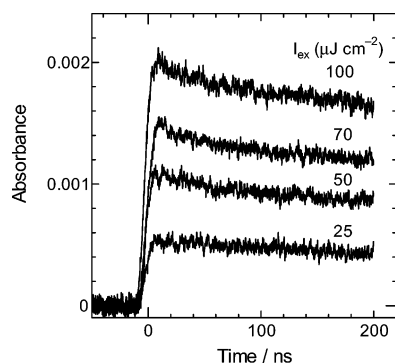


Figure 4. Temporal profiles of transient absorption of NKX-2311/ZnO observed at 1020 nm at four different exciting light intensities ($I_{\text{ex}} = 25, 50, 70$, and $100 \mu\text{J cm}^{-2}$).

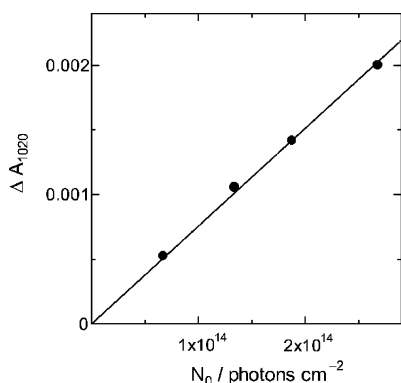


Figure 5. Absorbance change at 1020 nm just after excitation as a function of the number of incident excitation photons (N_0).

absorbance change of NKX-2311⁺ at 1020 nm at 0 ns (ΔA_{1020}) was linearly related to the number of incident excitation photons (Figure 5). The value of Φ_{inj} can be determined using eq 2. For the samples used here, the optical density at 532 nm was greater than 2; that is, the light-harvesting efficiency ($1 - T$) was almost unity. Thus, the absolute value of the efficiency of electron injection from excited NKX-2311 into the ZnO film can be estimated as 0.8 ± 0.1 .

The efficiency of electron injection is sensitive to I_{ex} .^{24,25} We found that the relative efficiency of electron injection decreases with increasing I_{ex} above $100 \mu\text{J cm}^{-2}$ in the ZnO system.²⁶ Below this intensity, the number of injection events per particle is estimated to be less than unity. This implies that a high-density excitation effect efficiently occurs when more than two injection events occur simultaneously in the same particle. Thus, injection events probably occur independently below a light intensity of $100 \mu\text{J cm}^{-2}$, suggesting that the same efficiency of electron injection can be expected under very weak excitation conditions, such as sunlight irradiation.

Previously, we determined the relative injection efficiencies of various sensitizer dyes adsorbed on ZnO films by comparing the absorbance due to conducting electrons of ZnO.²⁶ Figure 6 shows the transient absorption spectra of NKX-2311/ZnO and N3/ZnO. These spectra are normalized on the longer wavelength side because conducting electrons are products in both systems. For N3/ZnO, the absorption peak at 780 nm can be assigned to the oxidized form of the N3 dye produced by electron injection into the conduction band of the ZnO film.²⁶ The molar absorption coefficient of the oxidized form of the N3 dye is $6000 \text{ mol}^{-1} \text{ dm}^3 \text{ cm}^{-1}$ at 780 nm (Figure 6). Since the oxidized dye and conducting electrons are produced in a 1:1 concentration ratio, the molar absorption coefficient of the conducting electrons in ZnO is $6000 \text{ mol}^{-1} \text{ dm}^3 \text{ cm}^{-1}$ at 2500 nm (Figure

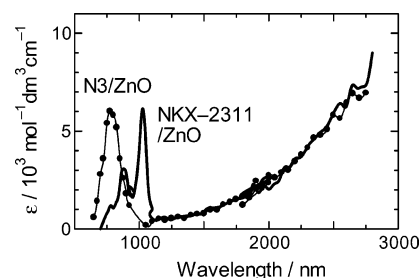


Figure 6. Transient absorption spectra of NKX-2311/ZnO (solid line) and N3/ZnO (closed circles).

6). From this value, the absolute value of the efficiency of electron injection for N3/ZnO can be estimated as 0.95 ± 0.15 . The same method can be used for other systems to estimate the absolute values of the injection efficiencies as well as the molar absorption coefficients. Recently, we determined the relative efficiencies of electron injection from excited N3 into various nanocrystalline semiconductors (TiO_2 , ZnO, Nb_2O_5 , SnO_2 , In_2O_3) films.⁴¹ Thus, the injection processes in these systems can be compared quantitatively.

Conclusion

The absolute value of the efficiency of electron injection from excited NKX-2311 into a nanocrystalline ZnO film was estimated as 0.8 ± 0.1 through transient absorption measurements. This value was obtained by using the molar absorption coefficient of oxidized NKX-2311, estimated by electron-transfer reaction in solution. The electron injection process in the dye-sensitized semiconductor surface can be quantitatively analyzed by comparing the absolute and relative efficiencies of electron injection.

Acknowledgment. We are grateful to Drs. Y. Ohga, S. Suga, and A. Sinpo (Hayashibara Biochemical Laboratories) for synthesis of NKX-2311 dyes. This work was supported by the New Energy and Industrial Technology Development Organization (NEDO). Additional support was provided by the COE development program and by a Grant-in-Aid for Scientific Research from the Ministry of Education, Culture, Sports, Science and Technology (MEXT) of Japan.

References and Notes

- (1) Nazeeruddin, M. K.; Kay, A.; Rodicio, I.; Humphry-Baker, R.; Muller, E.; Liska, P.; Vlachopoulos, N.; Grätzel, M. *J. Am. Chem. Soc.* **1993**, *115*, 6382–6390.
- (2) Islam, A.; Sugihara, H.; Arakawa, H. *J. Photochem. Photobiol., A: Chem.* **2003**, *158*, 131–138.
- (3) Hara, K.; Sugihara, H.; Tachibana, Y.; Islam, A.; Yanagida, M.; Sayama, K.; Arakawa, H.; Fujihashi, G.; Horiguchi, T.; Kinoshita, T. *Langmuir* **2001**, *17*, 5992–5999.
- (4) Hara, K.; Sato, T.; Katoh, R.; Furube, A.; Ohga, Y.; Shinpo, A.; Suga, S.; Sayama, K.; Sugihara, H.; Arakawa, H. *J. Phys. Chem. B* **2003**, *107*, 597–606.
- (5) Hara, K.; Tachibana, Y.; Ohga, Y.; Shinpo, A.; Suga, S.; Sayama, K.; Sugihara, H.; Arakawa, H. *Sol. Energy Mater. Sol. Cells* **2003**, *77*, 89–103.
- (6) Hara, K.; Kurashige, M.; Ito, S.; Shinpo, A.; Suga, S.; Sayama, K.; Arakawa, H. *Chem. Commun.* **2003**, 252–253.
- (7) Hara, K.; Kurashige, M.; Dan-oh, Y.; Kasada, C.; Shinpo, A.; Suga, S.; Sayama, K.; Arakawa, H. *New J. Chem.* **2003**, *27*, 783–785.
- (8) Tachibana, Y.; Moser, J. E.; Grätzel, M.; Klug, D. R.; Durrant, J. R. *J. Phys. Chem.* **1996**, *100*, 20056–20062.
- (9) Tachibana, Y.; Haque, S. A.; Mercer, I. P.; Durrant, J. R.; Klug, D. R. *J. Phys. Chem. B* **2000**, *104*, 1198–1205.
- (10) Tachibana, Y.; Haque, S. A.; Mercer, I. P.; Moser, J. E.; Klug, D. R.; Durrant, J. R. *J. Phys. Chem. B* **2001**, *105*, 7424–7431.

- (11) Tachibana, Y.; Rubtsov, I. V.; Montanari, I.; Yoshihara, K.; Klug, D. R.; Durrant, J. R. *J. Photochem. Photobiol., A: Chem.* **2001**, *142*, 215–220.
- (12) Hannappel, T.; Burfeindt, B.; Storck, W.; Willig, F. *J. Phys. Chem. B* **1997**, *101*, 6799–6802.
- (13) Asbury, J. B.; Ellingson, R. J.; Ghosh, H. N.; Ferrere, S.; Nozik, A. J.; Lian, T. *J. Phys. Chem. B* **1999**, *103*, 3110–3119.
- (14) Benkö, G.; Hilgendorff, M.; Yartsev, A. P.; Sundström, V. *J. Phys. Chem. B* **2001**, *105*, 967–974.
- (15) Benkö, G.; Kallioinen, J.; Korppi-Tommola, J. E. I.; Yartsev, A. P.; Sundström, V. *J. Am. Chem. Soc.* **2002**, *124*, 489–493.
- (16) Bauer, C.; Boschloo, G.; Mukhtar, E.; Hagfeldt, A. *J. Phys. Chem. B* **2001**, *105*, 5585–5588.
- (17) Asbury, J. B.; Wang, Y.; Lian, T. *J. Phys. Chem. B* **1999**, *103*, 6643–6647.
- (18) Furube, A.; Katoh, R.; Hara, K.; Murata, S.; Arakawa, H.; Tachiya, M. *J. Phys. Chem. B* **2003**, *107*, 4162–4166.
- (19) Iwai, S.; Hara, K.; Murata, S.; Katoh, R.; Sugihara, H.; Arakawa, H. *J. Chem. Phys.* **2000**, *113*, 3366–3373.
- (20) Kamat, P. V.; Bedja, I.; Hotchandani, S.; Patterson, L. K. *J. Phys. Chem. B* **1996**, *100*, 4900–4908.
- (21) Asbury, J. B.; Hao, E.; Wang, Y.; Ghosh, H. N.; Lian, T. *J. Phys. Chem. B* **2001**, *105*, 4545–4557.
- (22) Bauer, C.; Boschloo, G.; Mukhtar, E.; Hagfeldt, A. *Int. J. Photochem.* **2002**, *4*, 17–20.
- (23) Benkö, G.; Myllyperkiö, P.; Pan, J.; Yartsev, A. P.; Sundström, V. *J. Am. Chem. Soc.* **2002**, *124*, 1118–1119.
- (24) Kelly, C. A.; Farzad, F.; Thompson, D. W.; Stipkala, J. M.; Meyer, G. J. *Langmuir* **1999**, *15*, 7047–7054.
- (25) Kelly, C. A.; Meyer, G. J. *Coord. Chem. Rev.* **2001**, *211*, 295–315.
- (26) Katoh, R.; Furube, A.; Hara, K.; Murata, S.; Sugihara, H.; Arakawa, H.; Tachiya, M. *J. Phys. Chem. B* **2002**, *106*, 12957–12964.
- (27) Hara, K.; Horiuchi, H.; Katoh, R.; Singh, L. P.; Sugihara, H.; Sayama, K.; Murata, S.; Tachiya, M.; Arakawa, H. *J. Phys. Chem. B* **2002**, *106*, 374–379.
- (28) Horiuchi, H.; Katoh, R.; Hara, K.; Yanagida, M.; Murata, S.; Sugihara, H.; Arakawa, H.; Tachiya, M. *J. Phys. Chem. B* **2003**, *107*, 2570–2574.
- (29) Karstens, T.; Kobs, K. *J. Phys. Chem.* **1980**, *84*, 1871–1872.
- (30) Peover, M. E. *J. Chem. Soc.* **1962**, 4540–4549.
- (31) Nishimura, Y.; Sakuragi, H.; Tokumaru, K. *Bull. Chem. Soc. Jpn.* **1992**, *65*, 2887–2893.
- (32) Shida, T. *Electronic Absorption Spectra of Radical Ions*; Elsevier: Amsterdam, 1988.
- (33) Häupl, T.; Lomoth, R.; Hammarström, L. *J. Phys. Chem. B* **2003**, *107*, 435–438.
- (34) Meisel, D.; Mulac, W. A.; Matheson, M. S. *J. Phys. Chem.* **1981**, *85*, 179–187.
- (35) Das, S.; Kamat, P. V. *J. Phys. Chem. B* **1998**, *102*, 8954–8957.
- (36) Hannappel, T.; Burfeindt, B.; Storck, W.; Willig, F. *J. Phys. Chem. B* **1997**, *101*, 6799–6802.
- (37) Moser, J. E.; Noukakis, D.; Bach, U.; Tachibana, Y.; Klug, D. R.; Durrant, J. R.; Humphry-Baker, R.; Grätzel, M. *J. Phys. Chem. B* **1998**, *102*, 3649–3650.
- (38) Hannappel, T.; Zimmermann, C.; Meisser, B.; Burfeindt, B.; Storck, W.; Willig, F. *J. Phys. Chem. B* **1998**, *102*, 3651–3652.
- (39) Pankove, J. I. *Optical Processes in Semiconductors*; Dover: New York, 1975.
- (40) Haque, S. A.; Tachibana, Y.; Willis, R. L.; Moser, J. E.; Grätzel, M.; Klug, D. R.; Durrant, J. R. *J. Phys. Chem. B* **2000**, *104*, 538–547.
- (41) Katoh, R.; Furube, A.; Yoshihara, T.; Hara, K.; Fujihashi, G.; Takano, S.; Murata, S.; Arakawa, H.; Tachiya, M. *J. Phys. Chem. B*, submitted.